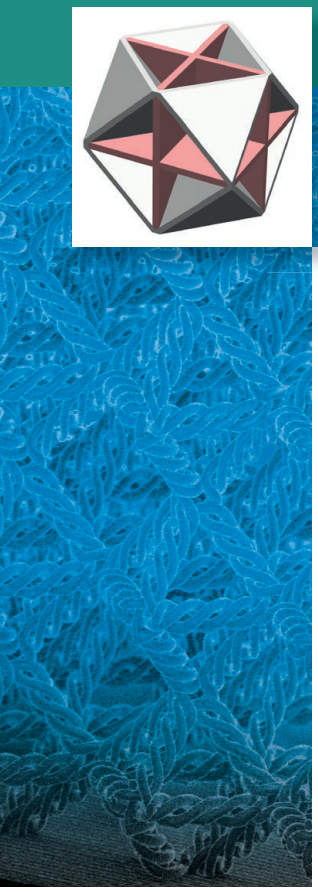


The extreme mechanics of micro- and nanoarchitected materials

R. Schwaiger, L.R. Meza, and X. Li

A material's properties are derived from its constituent material composition and its structural hierarchy across length scales down to the nanometer level. At submicron length scales, materials exhibit unique size-affected mechanical properties such as enhanced strength, ductility, and flaw tolerance, but these are generally lost in bulk materials. Emerging fabrication methods have enabled the creation of materials with controllable architectures down to the nanoscale. These micro- and nanoarchitected materials utilize both resilient architectures and size-affected constituent materials to achieve unprecedented mechanical properties such as ultrahigh strength at low density, recoverability after large applied strains in intrinsically brittle materials, and metamaterial properties such as chirality and negative static compressibility. In this article, we describe the governing principles behind these materials and outline recent progress in the field. We unravel the details of the deformation and failure processes to facilitate a fundamental understanding of effective materials properties and provide a guideline for the design of the next generation of nanoarchitected materials.

Introduction

Micro- and nanoarchitected materials represent a new class of materials with rationally designed structural hierarchy down to the nanoscale. These materials are capable of achieving extreme mechanical and metamaterial properties. Architecture, constituent materials, and architectural feature sizes, which allow for exploiting material size effects, define the mechanical properties. The introduction of controlled micro- and nanoarchitecture allows for the creation of materials with properties that far exceed those of their bulk counterparts, such as strengths greater than 1 GPa with densities below that of water, deformability, recoverability despite being made from intrinsically brittle constituents, and an insensitivity to large flaws. Multiple hierarchical structures can be introduced to control material deformation, similar to what is observed in biological materials.[1]

The mechanical behavior of an architected material can be decoupled into its material behavior and its architectural behavior. Architecture is responsible for properties such as high specific stiffness, "ductility" caused by structural instabilities, and most metamaterial properties[2] such as negative Poisson's ratio (auxetic behavior) and near infinite bulk to shear modulus ratio (pentamode stiffness). Architectural behavior is scale independent, meaning two identical architectures of different sizes with identical constituent material properties will have the same behavior. Metamaterial behaviors describe a subset of architectural behaviors and are both scale- and material-independent.

The advantage of micro- and nanoarchitected materials is that their constituent materials experience size-affected property changes that are utilized to improve the overall mechanical response. Mechanisms governing the size effects are complex, but there is a general overall trend of "smaller is stronger."[3,4] In addition, macroscopically brittle materials experience an enhanced ductility at the nanoscale[5] and materials such as metal nanowires have been observed to have notch insensitivity, resulting in the same failure strength independent of whether failure occurred at the notch or in the unnotched material.[6,7] Microstructural and dimensional constraints can significantly change the mechanical,[3,4,8] magnetic,[8] thermal,[9] and electrical[10] properties of a material relative to its bulk properties.

The field of mechanical metamaterials has benefited strongly from advances in three-dimensional (3D) additive manufacturing with light-based methods.[11] Techniques such as projection micro-stereolithography (PμSL)[12] and direct laser writing (DLW)[13,14] provide control over complicated 3D geometries with the nanoscale feature sizes necessary for

R. Schwaiger, Institute of Energy and Climate Research IEK-2, Forschungszentrum Jülich GmbH, and Institute for Applied Materials, Karlsruhe Institute of Technology (KIT), Germany; ruth.schwaiger@kit.edu
L.R. Meza, University of Washington, USA; lmeza@uw.edu
X. Li, Department of Engineering Mechanics, Tsinghua University, China; xiaoyanlithu@tsinghua.edu.cn
doi:10.1557/mrs.2019.230

© 2019 Materials Research Society
https://doi.org/10.1557/mrs.2019.230 Published online by Cambridge University Press

high-performance nanoarchitected materials. By combining these techniques with different post-processing approaches such as coating deposition or pyrolysis, the initially polymeric structures can be converted to composites, ceramics, or metals.[15] A large variety of micro- and nanoarchitected materials with unit cell sizes below 1 μm have been reported in recent years.[15] Other techniques such as holographic lithography[16] and self-assembly[17] have shown remarkable capabilities for creating nanoarchitectures with submicron features, and have demonstrated novel mechanical properties,[18,19] but offer limited control over changing the nanoscale structures.

In this article, we build upon comprehensive review articles on architected,[20,21] and micro- and nanoarchitected materials.[15,22] We focus on selected aspects of current interest in the field starting with architecture, exploring the role of size-affected material properties and elucidating how those can be effectively combined to bring about novel mechanical behavior.

High-strength, lightweight architected materials

The role of architecture

Manipulating the architecture or microstructural geometry[15,23,24] can effectively alter the mechanical behavior of architected materials and significantly expand the material design space. Architectures are classified as truss-, plate-, and shell-based with periodic or stochastic cellular structures. In contrast to the stochastic structures, the periodic ones offer greater potential to improve the efficiency in mechanical properties due to the ordered and regular arrangement of internal pores.[24]

For truss-based lattices, the common periodic unit cells include the octet-truss, iso-truss, 3D kagome, cuboctahedron, tetrahedron, and tetrakaidecahedron[25–28] (**Figure 1**a–c). These unit cells have different degrees of rigidity and nodal connectivity,[25] which mainly determine the mechanical response. Considering the deformation mode of a single strut, the truss-based lattice architectures are generally classified as stretching- and bending-dominated. In the ideal stretching-dominated one, each strut is subjected to uniaxial tension or compression (Figure 1a, c). However, in the real stretching-dominated lattice, the struts might experience local buckling, especially under a large strain. The bending-dominated lattice deforms via bending or buckling of single struts (Figure 1b). As a typical bending-dominated lattice, the tetrakaidecahedron lattice exhibits large deformability and good recoverability.[25] Under large compressive strain, it accommodates the deformation by local deformation at nodes, which makes these lattices sensitive to nodal compliance or imperfections.[25]

As a representative of stretching-dominated lattices, the octet-truss lattice exhibits good specific mechanical properties, but apparent anisotropies in both elastic modulus and yield strength.[28] Young's modulus in the [111] direction of the octet-truss lattice is maximum, while the compressive strength in both [111] and [001] directions are maximum over all directions.[28] Topology optimization based on finite element modeling showed that the iso-truss is isotropic and has optimal stiffness compared to other lattice topologies.[26] Recent experimental and computational studies[27] further demonstrated that the iso-truss lattice has better flaw tolerance than the lattices with octet-truss and tetrahedron unit cells, due to its better load-bearing and load-transfer ability.

Recently, plate-based lattices, replacing the struts with plates on the close-packed planes of crystalline structures, have emerged.[29,30] Based on finite element modeling and theoretical analyses, a design map was developed for the elastically isotropic plate-based lattice with cubic symmetry[30] (Figure 1d–e). The stiffness of these plate-based lattices is at

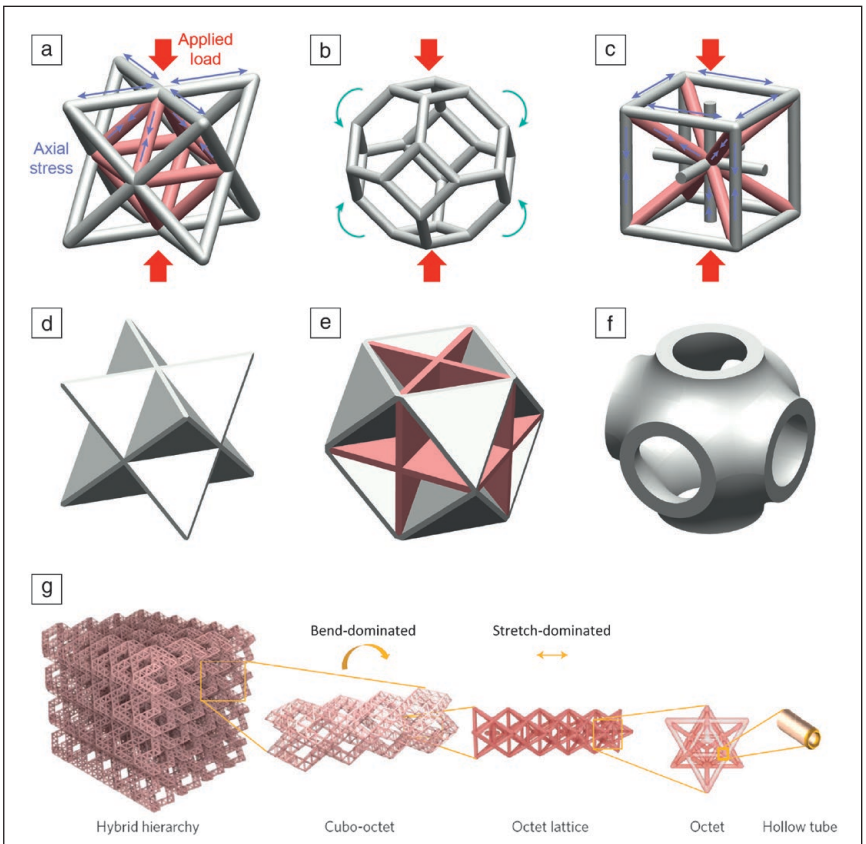


Figure 1. Schematic illustrations of typical unit cells of truss-, plate-, and shell-based lattices. (a) Octet-truss; (b) tetrakaidecahedron; (c) iso-truss; (d) octet unit cell for plate-based lattice; (e) hybrid unit cell of cubic and octet structures for plate-based lattice; (f) triply periodic minimal surface-like unit cell for shell-based lattice; (g) structural hierarchy of architected materials. Reprinted with permission from Reference 34. © 2016 Nature Publishing Group. The arrows in (a–c) indicate the load transfer and deformation mode of struts in the truss-based lattices.

https://doi.org/10.1557/mrs.2019.230 Published online by Cambridge University Press

least 3× higher than that of the stiffest truss-based lattices of equal mass.[30] These plate-based lattices are well-distributed networks of plates, which have more efficient loading transfer than the truss-based lattices with similar geometries.[29,30] Notably, a plate-based lattice with a combination of cubic and octet topologies has achieved the Hashin–Shtrikman upper bound,[29] which is a theoretical limit for the modulus of isotropic porous materials.

A novel shell-based lattice has been conceived by replacing the hollow truss with a continuous and curved shell.[31,32] In shell-based lattices, the nodes are interconnected through smooth shells, which reduce stress concentration around the nodes. Based on topology optimization, the curved shell is indeed a triply periodic minimal surface (TPMS),[31] which has a constant mean curvature at every point on the surface (Figure 1f). Shell-based lattices consisting of TPMS are stretching-dominated and experience coplanar stresses.[31] The shell-based lattices with well-developed interconnections are less sensitive to flaws than truss-based lattices with similar geometries, but show only little improvement in strength, because local buckling dominates the deformation.[31] By optimizing the shape or size of the shells, and by suppressing local buckling mechanisms, the mechanical properties of shell-based lattices can be further improved.

Inspired by hierarchical natural materials (e.g., bone, wood, and conch shell), hierarchy has been introduced into the design of architected materials.[33,34] 3D hierarchical architected materials consist of self-similar or dissimilar unit cells at different hierarchical levels with feature sizes spanning several orders of magnitude[33,34] (Figure 1g). Such a hierarchical design can expand the building volume without sacrificing structural integrity and improve mechanical properties by combining the benefits of microarchitectures at successive length scales. Therefore, such hierarchical structures reach into the ultralow density material property spaces (**Figure 2**). Because of the decoupling of strut length effective for Euler buckling (i.e., buckling of a monolithic beam under compression) and the relative density,[15] hierarchical architected materials exhibit improved buckling resistance and recoverability[15,33,34] facilitating linear scaling of compressive strength with relative density.

Exploiting material size effects

Material size effects are generally observed when extrinsic feature sizes approach the atomic scale and the continuum assumption of materials becomes invalid.[3,4,7] We focus here on size effects in mechanical properties, the most significant of which are enhanced strength[3,4,7] and ductility.[35] Although these novel nanomaterial properties are generally lost in bulk materials, careful control over nanoscale features enables them to be utilized in micro- and nanoarchitected materials.

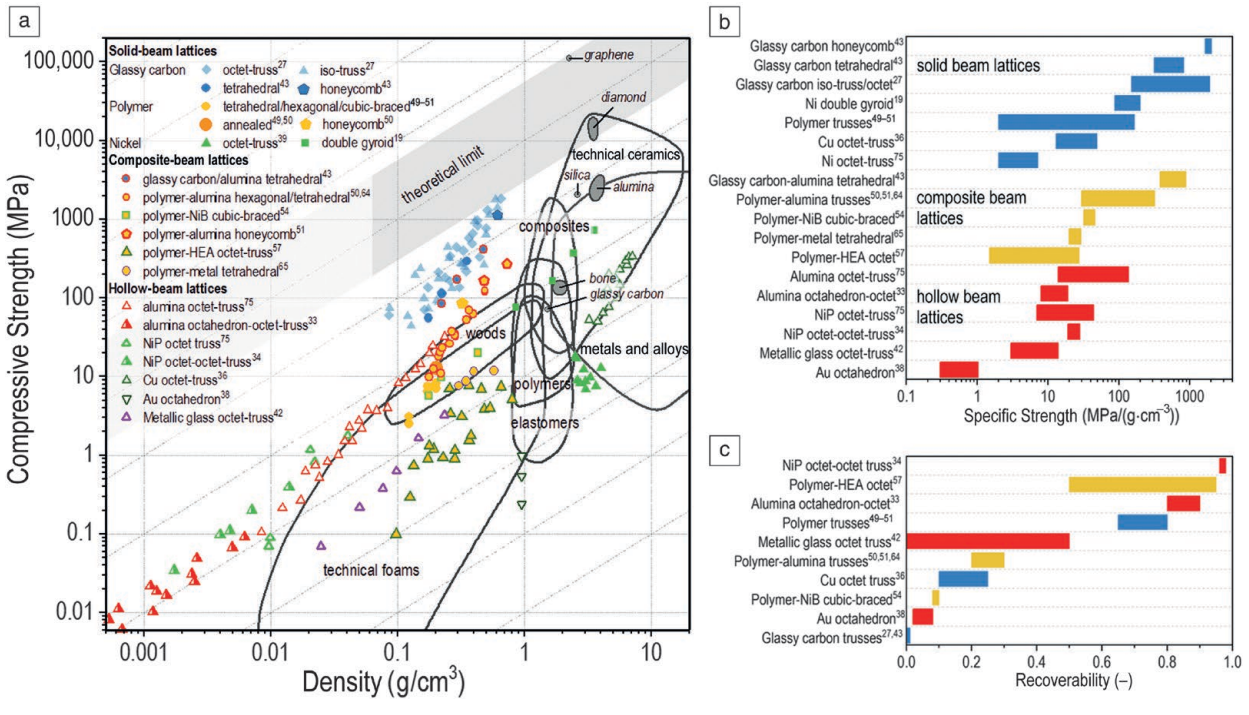


Figure 2. Strength and recoverability of existing micro- and nanoarchitected materials. (a) Material property chart showing compressive strength versus density. Many architected materials fill the empty spaces not accessible by known materials. For graphene,[48] the tensile strength has been included. (b) Glassy carbon and different composite-beam lattices reach the highest specific strengths, while such a clear advantage is not observed for the (c) recoverability. The lattices were deformed to different strain levels, but the high-entropy alloy (HEA)-coated structures still appear superior at combining high strength and recoverability underlining the importance of materials selection and architectural design.

https://doi.org/10.1557/mrs.2019.230 Published online by Cambridge University Press

Nanoscale strengthening is dependent upon both the constituent material system and its corresponding crystal or grain structure. In single-crystalline metals, size-effected strengthening can arise due to dislocation starvation, dislocation source truncation, and the elimination of "weakest-link" sources.[4] In micro- and nanoarchitected materials, this is seen predominantly, for instance, in electrodeposited copper mesolattices with strengths greater than that of bulk copper, despite having 50% of the latter's density,[36] and electrodeposited nickel double gyroid structures that have strengths equal to or greater than that of bulk nickel despite having just 38% of the bulk density.[19] Similar behaviors have been observed in nanoporous metals.[37]

Nanocrystalline metals conversely experience a smaller-is-weaker trend due to the enhanced mobility of grain boundaries at free surfaces. This is observed in sputtered gold nanolattices where structures with smaller features are weaker than structures with larger features at the same overall density[38] and, to some degree, in directly additive-manufactured pyrolyzed premetallic photopolymer nickel systems.[39] In ceramics and other intrinsically brittle materials, strength is traditionally governed by flaws via a "weakest link" mechanism that can be well characterized using a Weibull statistical distribution.[40,41] This has the effect of strengthening many nanoarchitected materials systems, for instance enabling metamaterial recoverability in nanolattices made from atomic-layer-deposited (ALD) aluminum oxide (Al_2O_3)[33,42] and ultrahigh strength in lightweight nanolattices made from pyrolyzed carbon.[27,43] Nanoscale strengthening also has a unique effect on the flaw tolerance of nanoarchitected materials. It has been observed that ALD Al_2O_3 nanolattices tested in tension are insensitive to notches[44] and pyrolyzed carbon nanolattices exhibit large strains to failure due to insensitivity to flaws of their constituent beams.[27]

Ductility can be enhanced at the nanoscale due to the availability of free surfaces, and the damage state at the free surfaces often drives the extent of ductility.[35] This effect is most pronounced in brittle materials such as silicon, ceramics, and metallic glasses, wherein ductility is enabled when feature sizes are smaller than the intrinsic size necessary for failure nucleation (e.g., shear transformation zones in metallic glass that are ~100 nm). The exploitation of enhanced ductility can be seen in nanolattices made from sputtered metallic glasses that suppress brittle failure when their feature sizes are reduced below ~50 nm.[45,46] It is also observed in copper nanolattices with a ~250-nm-thick coating of chemical-vapor-deposited (CVD) silicon that resists cracking during lithiation.[47] Although the previously mentioned results show promise for the enhancement of ductility using size effects in nanoarchitected materials, it is still an underutilized phenomenon.

Combining high strength and recoverability

Micro- and nanoarchitected materials combine specific architecture and size-dependent material properties to achieve superior macroscale properties. Because of their enhanced flaw tolerance at small length scales and increased yield strengths, they also have the potential to resolve the conflict between strength and deformability as commonly observed in bulk materials. Ideally, a material should be able to recover from deformation without significant structural degradation and repeatedly absorb mechanical energy. Solid materials that dissipate mechanical energy usually exploit viscoelasticity (i.e., internal material damping), as well as plasticity and fracture. By introducing appropriate architecture, additional mechanisms can occur such as elastic buckling and hysteretic instabilities (e.g., snap-through in a two-bar truss). While such scale-independent metamaterial mechanisms enable large deformations, the combination with nanoscale constituent materials will enhance deformability and energy dissipation.

Figure 2 summarizes the strength and recoverability of micro- and nanoarchitectures. The compressive strength versus density plot (Figure 2a) comprises a wide range of architectures and constituent materials together with the properties of common bulk materials. The strongest existing materials, here taken to be diamond and graphene,[48] define the theoretical strength limit, and the materials that have the same specific strength (i.e., strength-to-density ratio) will lie along the same dashed diagonal line in the strength versus density plot. Glassy carbon nanoarchitectures[27,43] with strength values above 1000 MPa have the highest specific strength of all nanoarchitected materials to date and almost reach the specific strength of diamond. Overall, the specific strengths of several lattices (Figure 2b), in particular the polymeric ones[49,50] and polymer-alumina composites,[50,51] reach or outperform the strengths of bulk metals. At very low densities <0.01 g cm^{-3}, hollow-beam octet architectures[42,76] and hierarchical structures[33,34] are significantly lighter than the foams and can reach a specific strength comparable to bulk metals and alloys.

Solid-beam microlattices often exhibit a high initial maximum stress when tested in compression,[50,52–54] followed by post-yield softening and a stress plateau with only little recovery upon unloading. The energy dissipation is significant though, and is mainly related to fracture and plastic deformation resulting in reduced recoverability. The higher the plateau stress in a loading cycle, the higher the energy dissipation. Hollow-beam micro- and nanolattices have shown impressive recovery of almost 100% of the applied strain even after compressive deformation up to 80% (Figure 2c).[33,42,55,56] Such behavior was not only observed for nickel alloy structures,[56] but also for alumina lattices.[42] However, recoverability of cellular materials is related inversely to the density and, thus, the enhanced recoverability of hollow-beam lattices is accompanied by relatively low strength values not much higher than those of foam materials of comparable densities. Composite micro- and nanolattices appear to be most effective in achieving high strength, together with good recoverability[54,57] (Figure 2b–c). Figure 2c should be interpreted cautiously, since the structures were deformed to somewhat different strain levels.

Elastic buckling is probably the most important mechanism for recoverability and energy absorption in micro- and nanolattices. Depending on the ratio of the wall thickness to the strut diameter, the deformation in thin-walled struts is

https://doi.org/10.1557/mrs.2019.230 Published online by Cambridge University Press

recoverable; shell buckling and low-stress hinges accommodate large macroscopic strain.[42,56] For buckling to dominate, the beams must be slender. To allow for shell buckling, the relative densities must be low. Buckling also contributes to strength, energy dissipation, and recovery of composite micro- and nanoarchitectures.[50,54,57] Stretching-dominated polymer lattices with strut diameters of 1 μm coated with 10-nm NiB showed delayed buckling since the coating confined the polymer core, providing added strength. Extended plastic deformation or a plateau regime with partial recovery was observed for 10-nm NiB coatings, while for 100-nm-thick NiB coatings, brittle failure occurred.[54] For octet-truss lattices consisting of thinner struts of 500-nm diameter coated with a high entropy alloy,[57] the elastic buckling allowed for pronounced rotation of the nodes. High recovery even after 50% compressive strain was observed,[57] while still maintaining a specific strength that reached 50% of the specific strength of alumina-coated composite lattices.[50] The optimal coating thickness was identified to be 14–50 nm since thicker coatings resulted in fracture rather than buckling and node rotation.[57]

Deformation and failure behavior

Local deformation and failure

The mechanical properties of architected materials depend on the local tensile, compressive, and shear loading states. The corresponding stiffness, strength, hardening/softening behavior, damage evolution, and strain limit of each can be set by the constituent material or by instabilities such as buckling, each of which can be extremely anisotropic and exhibit large tension–compression asymmetry.

Constituent material behavior is defined by atomic structure and corresponding deformation mechanisms. For example, carbon can form weakly bonded graphitic sheets (e.g., in carbon fiber having axial stiffness >10× its transverse stiffness),[58] or it can form amorphous carbon,[43] which is relatively isotropic in both strength and stiffness, but whose properties are affected by defect size and carbon bond configurations.[59] Brittle materials undergo catastrophic failure in both tension and compression (**Figure 3**c), and can be orders of magnitude weaker in tension because their strength is flaw-limited.[60] Brittle nanomaterials have minimal tension–compression asymmetry in strength due to the smaller number of defects,[40,41] although the tensile failure strain is still $\varepsilon_f \approx 5\%$ even for the strongest nanomaterials.[61]

Ductile materials generally have little tension–compression asymmetry, as their strength is governed by dislocation motion. For isolated ductile members, there is an emergent tension–compression asymmetry after the onset of plasticity because tension causes necking and a loss of integrity, while compression causes expansion and densification (Figure 3a–b).[34,62] Anisotropy in mechanical properties can have a significant effect on overall properties, but it has yet to be thoroughly

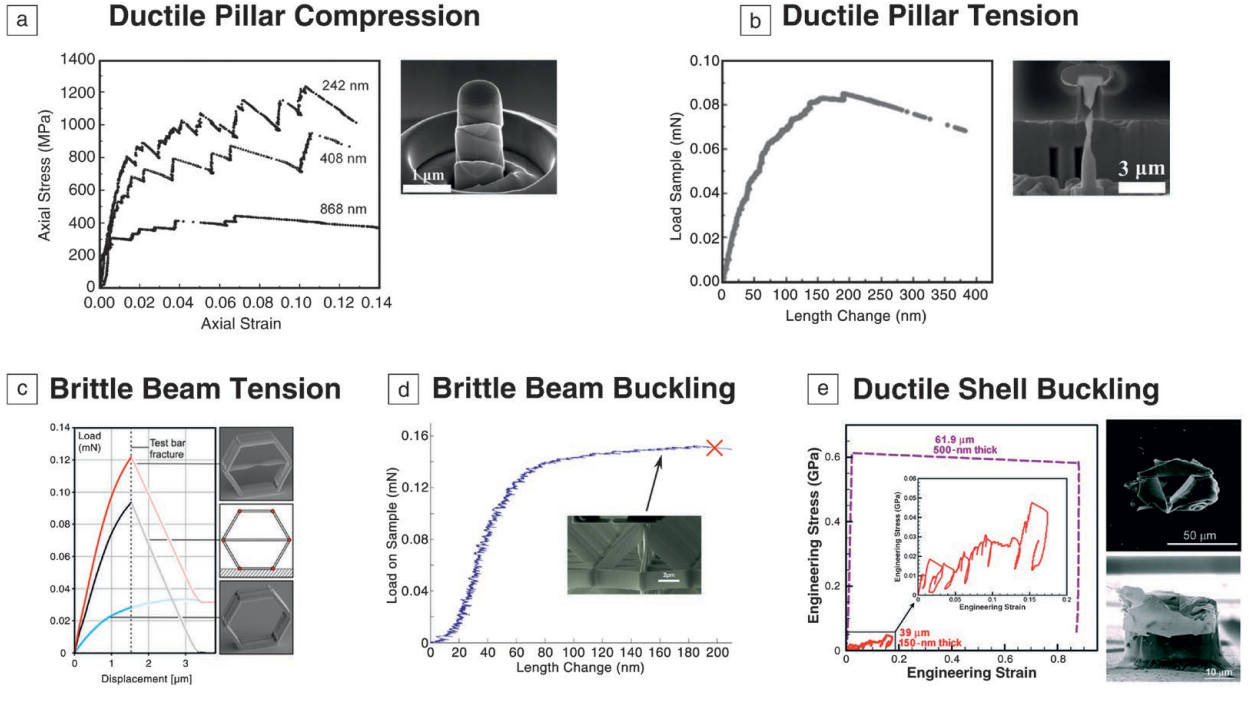


Figure 3. Local behaviors. (a) Compression of single-crystal niobium and (b) tension of single-crystal gold showing the inherent tension–compression asymmetry due to densification versus necking. Adapted with permission from Reference 62. © 2009 The Minerals, Metals & Materials Society. (c) Tension of an Al_2O_3 beam showing brittle response.[41] (d) Compression of four-bar hollow TiN beams showing buckling response.[63] (e) Catastrophic (pink) versus gradual (red) collapse of a hollow NiP cylinder due to shell buckling. Adapted with permission from Reference 71. © 2011 American Chemical Society.

https://doi.org/10.1557/mrs.2019.230 Published online by Cambridge University Press

studied or effectively utilized in tuning the mechanical properties of nanoarchitected materials.

While constituent materials properties are important, it is critical to consider the local distribution of stresses that emerge in various structures. Beams, plates, and shells can be loaded in pure tension or compression, but they often experience bending, which causes both tensile and compressive stresses. Brittle materials in bending will fail catastrophically when the tensile fracture stress is reached,[42,43,63] while ductile materials will generally form a plastic hinge and experience localized deformation.[36,38,55] Bending in structural members is a less significant factor in denser structures (with >5–10% relative density), because the intersections between beams and plates at nodes and joints contribute considerably to the load-carrying ability and are much more significant sources of stress concentration.[25,64] Nodes are generally loaded in bending and have high stress concentrations, meaning they are often the initial point for failure.[42,43,65,66] Attempts to work around this issue by changing the node geometry have had minimal success,[64] while other types of spinodal structures[67] and minimal surface structures[68] have had more success by introducing architectures without any defined nodes.

Structural instabilities in lightweight architected materials have an effective material response. For example, slender beams made from brittle constituents have a brittle response in tension, but can bend or buckle in compression, thereby sustaining large deformations[40,63] (Figure 3d). This means that instabilities can generate a considerable tension–compression anisotropy. Instabilities occur in slender beam members via beam buckling, which occurs at a critical stress $\sigma_{cr} = \frac{\pi^2 EI}{A(kL)^2}$, where E is Young's modulus, I is the second moment of area, A is the area, L is the beam length, and k is a factor to account for boundary conditions.[69] Different types of lattices can create different effective boundary conditions, with more interconnected structures having a more fixed boundary ($k \approx 0.5$) and less connected structures having a more pinned boundary ($k \approx 1$).[70] It is convenient to describe a slenderness ratio.

$$\lambda = \sqrt{AL^2 / I}.$$

Instabilities in thin plates and shells occur via shell buckling. This type of buckling is extremely complex due to the numbers of buckling modes that can occur depending on the boundary conditions[71] (Figure 3e). The simplest case is for a thin hollow circular shell, for which the buckling limit is

$$\sigma_{cr} = \frac{E}{\sqrt{3(1-\nu^2)}}\left(\frac{t}{r}\right),$$

where v is the Poisson's ratio, t is the wall thickness, and r is the beam radius.[69] Buckling is an inherently elastic phenomenon, but it can result in high local stresses in buckled regions that lead to plastic deformation or failure. If the members are sufficiently slender, the post-buckled stress will not cause failure and structures can recover, as is seen in micro- and nanoarchitectures made from both ductile and brittle constituents[42,55,56] (Figure 2). This is better enabled in micro- and nanoarchitected materials due to the high stresses to failure of the constituent materials. However, residual plasticity or failure will reduce recovery and cause a prebuckled path that lowers the stress necessary to reinitiate buckling.

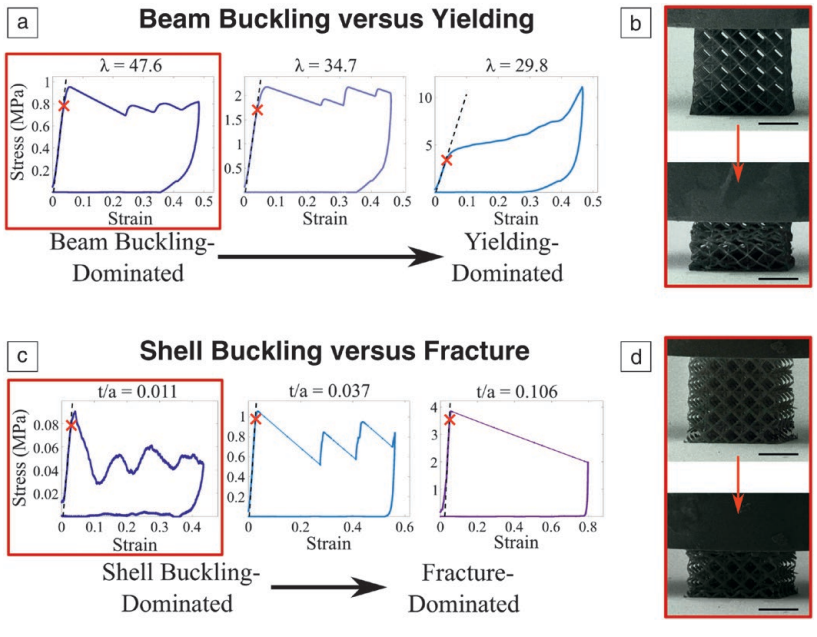


Figure 4. Global behaviors. (a) Transition from beam buckling to yielding-dominated behavior in a solid polymer cuboctahedron nanolattice with varying slenderness, λ, and (b) corresponding buckled state.[70] (c) Transition from shell buckling to fracture-dominated behavior in a hollow Al_2O_3 cuboctahedron nanolattice with varying thickness to semi-major ellipse axis ratio, t/a, and (d) corresponding shell buckled state.[70] (b, d) Scale bars = 20 μm.

Global deformation and failure

The architecture, applied load, and distribution of defects affect how load is transferred and correspondingly affect the emergent deformation and failure behavior of micro- and nanoarchitected materials. The compression behavior of lightweight architectures is dominated by the slenderness or aspect ratio of the constituent members. For architectures with non-slender beams or "thick" shells, their behavior will be yielding-dominated (i.e., governed by the plasticity of the constituents)[70] (**Figure 4**a, c). Yielding-dominated architectures with ductile constituents comprise a plateau region correlated with the onset of plasticity, which often starts at nodes and joints, and an eventual densification region when members contact one another.[25,34,36,38,39,55,72] The onset of densification occurs earlier for architectures with higher relative density.

https://doi.org/10.1557/mrs.2019.230 Published online by Cambridge University Press

Yielding-dominated architectures with brittle constituents undergo catastrophic collapse when the fracture strength of one of the members or nodes is reached.[27,43,45,51,63,65,73,74] For architectures with slender beams or "thin" shells, their behavior is governed by buckling of the members[70] (Figure 4). This buckling-dominated behavior depends on the structure and is generally ductile-like, independent of the properties of the constituent materials, making it a metamaterial behavior.[42,56] Buckling events lead to load drops that occur in a layer-by-layer manner, and the magnitude of the drops depends on the architecture.[12,33,46,55,56,70,75,76] The absolute slenderness of the constituents determines the residual yield or fracture in the members, which affects the recoverability.[42,55,56] This means that architectures with more slender members will be more recoverable and will display a more repeatable stress–strain response.[77]

The tension behavior of micro- and nanoarchitected materials is generally dominated by stress concentrations in the architecture, although this aspect is much less studied than compression. Tension in architectures made from ductile constituent beams and shells fail progressively and experience large load drops as individual members fail.[12] Tension in architectures made from brittle constituent beams and shells fail in a single catastrophic event.[44,65,78] In both, nodes serve as initiation points for failure because they are the source of highest stress concentration. Although there are architectures that minimize stress concentrations at nodes,[31,67] it is unlikely they would be a significant improvement on the overall tensile response. The progression of failure in architectures in tension causes a reduction in integrity as members begin to neck or fracture entirely, so measurements must be made in a displacement-controlled setup if they are to extract meaningful information before the onset of catastrophic failure.[12]

The imperfection landscape is somewhat overlooked, but it can strongly influence behaviors. Waviness in solid beams or hollow shells can significantly reduce the load-carrying capability of the individual members in compression and thereby the whole structure, particularly when the waviness is on the order of the member thickness.[25,33] Misaligned nodes, however, have a minimal effect on mechanical properties,[25] meaning architecture is more important to overall properties. Missing members can quickly degrade the properties of the architecture beyond the strength and stiffness scaling with density,[25,79] but the controlled distribution of missing members can potentially be used to improve deformation pathways and increase energy absorption.[80] Some architectures can even be insensitive to large imperfections such as missing beams, meaning they are highly flaw-tolerant and suggesting that the complex load carrying must be fully modeled and understood to predict behavior.[44] This flaw tolerance is not to suggest that micro- and nanoarchitectures are tough. On the contrary, it is predicted that the toughness of lattice materials scales with the square root of the unit cell size.[81] Thus, a structure with nanoscale beams would have a significantly lower toughness, although this has yet to be demonstrated experimentally for any sufficiently small (i.e., submillimeter-sized) sample.

Outlook

While the field of micro- and nanoarchitected materials has progressed rapidly over the past few years, their full potential remains to be explored. In this article, we highlighted the size-affected mechanical properties of micro- and nanoarchitected materials, but the inherent precision of nanoscale manufacturing is beneficial for other scale-independent metamaterial properties, such as pentamode meta-fluidity,[82,83] extremal auxetic behavior,[84] or tunable thermal expansion.[85] The field of 3D chiral mechanical metamaterials, which in the static case exhibit a twist upon compression and circularly polarized eigenstates in the dynamic case, is just emerging.[86–88] In addition to setting the new boundaries of material–property spaces, the introduction of micro- and nanoarchitecture facilitates programmability of mechanical properties,[89] making it possible to tailor stimulus-responsive, adaptive behavior depending on the loading situation. This should ultimately lead to the rational design of tailored properties.

Acknowledgments

R.S. acknowledges financial support from the Deutsche Forschungsgemeinschaft (DFG, German Research Foundation) under Germany's Excellence Strategy-2082/1-390761711. X.L. acknowledges financial support from the National Natural Science Foundation of China (Grant Nos. 11522218 and 11720101002).

References

1. P. Fratzl, R. Weinkamer, *Prog. Mater. Sci.* **52**, 1263 (2007).
2. A.A. Zadpoor, *Mater. Horiz.* **3**, 371 (2016).
3. O. Kraft, P.A. Gruber, R. Mönig, D. Weygand, *Annu. Rev. Mater. Res.* **40**, 293 (2010).
4. J.R. Greer, J.T.M. De Hosson, *Prog. Mater. Sci.* **56**, 654 (2011).
5. C. Koch, D. Morris, K. Lu, A. Inoue, *MRS Bull.* **24**, 54 (1999).
6. C. Ensslen, C. Brandl, G. Richter, R. Schwaiger, O. Kraft, *Acta Mater.* **108**, 317 (2016).
7. X.W. Gu, Z. Wu, Y.-W. Zhang, D.J. Srolovitz, J.R. Greer, *Nano Lett.* **13**, 5703 (2013).
8. E. Arzt, *Acta Mater.* **46**, 5611 (1998).
9. D. Josell, S.H. Brongersma, Z. Tökei, *Annu. Rev. Mater. Res.* **39**, 231 (2009).
10. A.J. Minnich, J.A. Johnson, A.J. Schmidt, K. Esfarjani, M.S. Dresselhaus, K.A. Nelson, G. Chen, *Phys. Rev. Lett.* **107**, 095901 (2011).
11. I. Gibson, D.W. Rosen, B. Stucker, *Additive Manufacturing Technologies* (Springer, New York, 2015).
12. X. Zheng, J. Deotte, M.P. Alonso, G.R. Farquar, T.H. Weisgraber, S. Gemberling, H. Lee, N. Fang, C.M. Spadaccini, *Rev. Sci. Instrum.* **83**, 125001 (2012).
13. S. Maruo, O. Nakamura, S. Kawata, *Opt. Lett.* **22**, 132 (1997).
14. T. Baldacchini, *Three-Dimensional Microfabrication Using Two-Photon Polymerization*, 1st ed. (Elsevier, Amsterdam, The Netherlands, 2015).
15. J. Bauer, L.R. Meza, T.A. Schaedler, R. Schwaiger, X. Zheng, L. Valdevit, *Adv. Mater.* **29**, 1701850 (2017).
16. T. Jeon, D.-H. Kim, S.-G. Park, *Adv. Mater. Interfaces* **5**, 1800330 (2018).
17. W. Bai, C.A. Ross, *MRS Bull.* **41**, 100 (2016).
18. J.J. do Rosário, E.T. Lilleodden, M. Waleczek, R. Kubrin, A.Y. Petrov, P.N. Dyachenko, J.E.C. Sabisch, K. Nielsch, N. Huber, M. Eich, G.A. Schneider, *Adv. Eng. Mater.* **17**, 1420 (2015).
19. S.N. Khaderi, M.R.J. Scherer, C.E. Hall, U. Steiner, U. Ramamurty, N.A. Fleck, V.S. Deshpande, *Extreme Mech. Lett.* **10**, 15 (2017).
20. L. Montemayor, V. Chernow, J.R. Greer, *MRS Bull.* **40**, 1122 (2015).
21. T.A. Schaedler, W.B. Carter, *Annu. Rev. Mater. Res.* **46**, 187 (2016).
22. X. Zhang, Y. Wang, B. Ding, X. Li, *Small* 1902842 (2019).
23. X. Yu, J. Zhou, H. Liang, Z. Jiang, L. Wu, *Prog. Mater. Sci.* **94**, 114 (2018).
24. S.J. Yeo, M.J. Oh, P.J. Yoo, *Adv. Mater.* **31**, 1803670 (2018).
25. L.R. Meza, G.P. Phlipot, C.M. Portela, A. Maggi, L.C. Montemayor, A. Comella, D.M. Kochmann, J.R. Greer, *Acta Mater.* **140**, 424 (2017).
26. M.C. Messner, *J. Mech. Phys. Solids* **96**, 162 (2016).

https://doi.org/10.1557/mrs.2019.230 Published online by Cambridge University Press

27. X. Zhang, A. Vyatskikh, H. Gao, J.R. Greer, X. Li, *Proc. Natl. Acad. Sci. U.S.A.* **116**, 6665 (2019).
28. T. Tancogne-Dejean, D. Mohr, *Int. J. Solids Struct.* **138**, 24 (2018).
29. J.B. Berger, H.N.G. Wadley, R.M. McMeeking, *Nature* **543**, 533 (2017).
30. T. Tancogne-Dejean, M. Diamantopoulou, M.B. Gorji, C. Bonatti, D. Mohr, *Adv. Mater.* **30**, 1803334 (2018).
31. B.D. Nguyen, J.S. Cho, K. Kang, *Mater. Des.* **95**, 490 (2016).
32. M.G. Lee, J.W. Lee, S.C. Han, K. Kang, *Acta Mater.* **103**, 595 (2016).
33. L.R. Meza, A.J. Zelhofer, N. Clarke, A.J. Mateos, D.M. Kochmann, J.R. Greer, *Proc. Natl. Acad. Sci. U.S.A.* **112**, 11502 (2015).
34. X. Zheng, W. Smith, J. Jackson, B. Moran, H. Cui, D. Chen, J. Ye, N. Fang, N. Rodriguez, T. Weisgraber, C.M. Spadaccini, *Nat. Mater.* **15**, 1100 (2016).
35. D.Z. Chen, D. Jang, K.M. Guan, Q. An, W.A. Goddard III, J.R. Greer, *Nano Lett.* **13**, 4462 (2013).
36. X.W. Gu, J.R. Greer, *Extreme Mech. Lett.* **2**, 7 (2015).
37. H.J. Jin, J. Weissmüller, D. Farkas, *MRS Bull.* **43**, 35 (2018).
38. L.C. Montemayor, J.R. Greer, *J. Appl. Mech.* **82**, 1 (2015).
39. A. Vyatskikh, S. Delalande, A. Kudo, X. Zhang, C.M. Portela, J.R. Greer, *Nat. Commun.* **9**, 593 (2018).
40. D. Jang, L.R. Meza, F. Greer, J.R. Greer, *Nat. Mater.* **12**, 893 (2013).
41. J. Bauer, A. Schroer, R. Schwaiger, I. Tesari, C. Lange, L. Valdevit, O. Kraft, *Extreme Mech. Lett.* **3**, 105 (2015).
42. L.R. Meza, S. Das, J.R. Greer, *Science* **345**, 1322 (2014).
43. J. Bauer, A. Schroer, R. Schwaiger, O. Kraft, *Nat. Mater.* **15**, 438 (2016).
44. L.C. Montemayor, W.H. Wong, Y.-W. Zhang, J.R. Greer, *Sci. Rep.* **6**, 1 (2016).
45. S.-W. Lee, M. Jafary-Zadeh, D.Z. Chen, Y.-W. Zhang, J.R. Greer, *Nano Lett.* **15**, 5673 (2015).
46. R. Liontas, J.R. Greer, *Acta Mater.* **133**, 393 (2017).
47. X. Xia, C.V. Di Leo, X.W. Gu, J.R. Greer, *ACS Energy Lett.* **1**, 492 (2016).
48. C. Lee, X. Wei, J.W. Kysar, J. Hone, *Science* **321**, 385 (2008).
49. A. Schroer, J. Bauer, R. Schwaiger, O. Kraft, *Extreme Mech. Lett.* **8**, 283 (2016).
50. A. Schroer, J.M. Wheeler, R. Schwaiger, *J. Mater. Res.* **33**, 274 (2018).
51. J. Bauer, S. Hengsbach, I. Tesari, R. Schwaiger, O. Kraft, *Proc. Natl. Acad. Sci. U.S.A.* **111**, 2453 (2014).
52. M.F. Ashby, *Philos. Trans. R. Soc. A* **364**, 15 (2006).
53. T.A. Schaedler, C.J. Ro, A.E. Sorensen, Z. Eckel, S.S. Yang, W.B. Carter, A.J. Jacobsen, *Adv. Eng. Mater.* **16**, 276 (2014).
54. M. Mieszala, M. Hasegawa, G. Guillonneau, J. Bauer, R. Raghavan, C. Frantz, O. Kraft, S. Mischler, J. Michler, L. Philippe, *Small* **13**, 1602514 (2017).
55. T.A. Schaedler, A.J. Jacobsen, A. Torrents, A.E. Sorensen, J. Lian, J.R. Greer, L. Valdevit, W.B. Carter, *Science* **334**, 962 (2011).
56. K.J. Maloney, C.S. Roper, A.J. Jacobsen, W.B. Carter, L. Valdevit, T.A. Schaedler, *APL Mater.* **1**, 022106 (2013).
57. X. Zhang, J. Yao, B. Liu, J. Yan, L. Lu, Y. Li, H. Gao, X. Li, *Nano Lett.* **18**, 4247 (2018).
58. E. Totry, J.M. Molina-Aldareguía, C. González, J. Llorca, *Compos. Sci. Technol.* **70**, 970 (2010).
59. A. Albiez, R. Schwaiger, *MRS Adv.* **4**, 133 (2019).
60. R. Danzer, P. Supancic, J. Pascual, T. Lube, *Eng. Fract. Mech.* **74**, 2919 (2007).
61. T. Zhu, J. Li, *Prog. Mater. Sci.* **55**, 710 (2010).
62. J.R. Greer, J.Y. Kim, M.J. Burek, *JOM* **61**, 19 (2009).
63. L.R. Meza, J.R. Greer, *J. Mater. Sci.* **49**, 2496 (2013).
64. C.M. Portela, J.R. Greer, D.M. Kochmann, *Extreme Mech. Lett.* **22**, 110 (2018).
65. J. Bauer, A. Schroer, R. Schwaiger, O. Kraft, *Adv. Eng. Mater.* **18**, 1537 (2016).
66. T. Juarez, A. Schroer, R. Schwaiger, A.M. Hodge, *Mater. Des.* **140**, 442 (2018).
67. M.T. Hsieh, B. Endo, Y. Zhang, J. Bauer, L. Valdevit, *J. Mech. Phys. Solids* **125**, 401 (2019).
68. S.C. Han, J.W. Lee, K. Kang, *Adv. Mater.* **27**, 5506 (2015).
69. S.P. Timoshenko, J.M. Gere, *Theory of Elastic Stability* (McGraw-Hill, New York, 1961).
70. L.R. Meza, "Design, Fabrication, and Mechanical Property Analysis of 3D Nanoarchitected Materials," PhD thesis, California Institute of Technology (2016).
71. J. Lian, D. Jang, L. Valdevit, T.A. Schaedler, A.J. Jacobsen, W.B. Carter, J.R. Greer, *Nano Lett.* **11**, 4118 (2011).
72. L. Valdevit, S.W. Godfrey, T.A. Schaedler, A.J. Jacobsen, W.B. Carter, *J. Mater. Res.* **28**, 2461 (2013).
73. Z.C. Eckel, C. Zhou, J.H. Martin, A.J. Jacobsen, W.B. Carter, T.A. Schaedler, *Science* **351**, 58 (2016).
74. H. Cui, R. Hensleigh, H. Chen, X. Zheng, *J. Mater. Res.* **33**, 360 (2018).
75. A. Torrents, T.A. Schaedler, A.J. Jacobsen, W.B. Carter, L. Valdevit. *Acta Mater.* **60**, 3511 (2012).
76. X. Zheng, H. Lee, T.H. Weisgraber, M. Shusteff, J. DeOtte, E.B. Duoss, J.D. Kuntz, M.M. Biener, Q.Q. Ge, J.A. Jackson, S.O. Kucheyev, N.X. Fang, C.M. Spadaccini, *Science* **344**, 1373 (2014).
77. L. Salari-Sharif, T.A. Schaedler, L. Valdevit, *J. Mater. Res.* **29**, 1755 (2014).
78. A.J. Mateos, W. Huang, Y.W. Zhang, J.R. Greer, *Adv. Funct. Mater.* **29**, 1806772 (2019).
79. A. Gross, P. Pantidis, K. Bertoldi, S. Gerasimidis, *J. Mech. Phys. Solids* **124**, 577 (2019).
80. Z. Vangelatos, K. Komvopoulos, C.P. Grigoropoulos, *Math. Mech. Solids* **24**, 511 (2019).
81. M.R. O'Masta, L. Dong, L. St-Pierre, H.N.G. Wadley, V.S. Deshpande, *J. Mech. Phys. Solids* **98**, 271 (2017).
82. M. Kadic, T. Bückmann, R. Schittny, P. Gumbsch, M. Wegener, *Phys. Rev. Appl.* **2**, 054007 (2014).
83. T. Bückmann, M. Thiel, M. Kadic, R. Schittny, M. Wegener, *Nat. Commun.* **5**, 4130 (2014).
84. S. Hengsbach, A. Díaz Lantada, *Smart Mater. Struct.* **23**, 087001 (2014).
85. J. Qu, M. Kadic, A. Naber, M. Wegener, *Sci. Rep.* **7**, 40643 (2017).
86. I. Fernandez-Corbaton, C. Rockstuhl, P. Ziemke, P. Gumbsch, A. Albiez, R. Schwaiger, T. Frenzel, M. Kadic, M. Wegener, *Adv. Mater.* **31**, 1807742 (2019).
87. T. Frenzel, M. Kadic, M. Wegener, *Science* **358**, 1072 (2017).
88. T. Frenzel, J. Köpfler, E. Jung, M. Kadic, M. Wegener, *Nat. Comm.* **29**, 3384 (2019).
89. T. Frenzel, C. Findeisen, M. Kadic, P. Gumbsch, M. Wegener, *Adv. Mater.* **28**, 5865 (2016). □



Ruth Schwaiger is the director of the Institute of Energy and Climate Research IEK-2 at Forschungszentrum Jülich GmbH, Germany. She conducted doctoral research at the Max-Planck-Institute for Metals Research in Stuttgart, Germany, and obtained her doctoral degree from the University of Stuttgart, Germany, in 2002. She completed postdoctoral research at the Massachusetts Institute of Technology and headed the Nanomechanics Research Group at the Karlsruhe Institute of Technology, Germany. Her current research interests include deformation mechanisms in materials, the mechanics of small-scale structures and nanoarchitected materials, and developing a mechanism-based understanding of deformation and failure. Schwaiger can be reached by email at ruth.schwaiger@kit.edu.



Lucas Meza is an assistant professor at the University of Washington. He leads a group investigating the mechanics of micro- and nanoarchitected materials. He was previously at the University of Cambridge, UK, where he was a research associate studying the micromechanical behavior of 3D woven fiber composites. He obtained his PhD degree in mechanical engineering at the California Institute of Technology in 2016. Meza can be reached by email at lmeza@uw.edu.



Xiaoyan Li is an associate professor in the Department of Engineering Mechanics, Tsinghua University, China. He received his PhD degree from Brown University in 2012. His research interests include the deformation and fracture of nanostructured materials (including nanocrystalline/nanotwinned materials and low-dimensional nanomaterials), design, fabrication, and mechanics of high entropy alloys and micro-/nanolattices, and development of multiscale modeling. He received the *Extreme Mechanics Letters* Young Investigator Award in 2018 and the Eshelby Mechanics Award for Young Faculty in 2018. Li can be reached by email at xiaoyanlithu@tsinghua.edu.cn.

https://doi.org/10.1557/mrs.2019.230 Published online by Cambridge University Press